Egyptian Journal of Chemistry

http://ejchem.journals.ekb.eg/

Utilization of Biodegradable Nanofiltration Membrane for Efficient Removal of Anionic Textile Dye

Ahmed Eteba[1,4], Mohamed Bassyouni[2,3,4*] , Medhat H. Elzahar[1], Mohamed Z. El-shekhiby[1]

[1] *Sanitary and Environmental Engineering, Department of Civil Engineering, Faculty of Engineering, Port Said University, Port Said 42526, Egypt.*

[2] *Department of Chemical Engineering, Faculty of Engineering, Islamic University of Madinah, Madinah, 42351, Saudi Arabia.*

[3] *Department of Chemical Engineering, Faculty of Engineering, Port Said University, Port Said 42526, Egypt.*

[4] *Centre of Excellence in Membrane-Based Water Desalination Technology for Testing and Characterization (CEMTC), Port Said University, Port Said 42526, Egypt.*

Abstract

Dye pollution has a major adverse effect on ecosystems and human health since it comprises complex pollutants containing dyestuff and chemicals. During the last period, some promising solutions to remove dyes from textile wastewater have come through separation technologies that are based on membranes. However, limitations have been identified with polymeric membranes due to their non-biodegradability and environmental impact. Chitosan-based membranes are getting more attention mainly because they are biocompatible, sustainable, and can be tailored for specific applications. Chitosan (CS) is a sustainable and biodegradable membrane material. In this study, a flat-membrane sheet of neat chitosan (CS) was fabricated using a solvent-casting process on nonwoven support (polyester) to prepare a multilayer composite nanofiltration membrane. The composite CS membrane was investigated by scanning electron microscope (SEM), contact angle measurements, atomic force microscopy (AFM), and mechanical testing. The characterization results showed improvements in surface roughness, hydrophilicity, tensile strength, and overall surface structure. By utilizing the multilayer technique during membrane fabrication, the membrane surface was transformed from a rough texture with large pore radii to a smooth surface featuring a refined pore structure. Furthermore, it exhibited a high rejection efficiency of 100 % for anionic direct blue 78 dye with permeation flux 9.3 $Lm^{-2}h^{-1}$ and excellent antifouling performance for a 600 min filtration test. These results showed that the CS nanofiltration membrane has a promising application for hazardous contaminants removal from textile dyeing effluent.

Keywords: Chitosan; Nanofiltration; Dye removal; Textile wastewater.

1. Introduction

Textile wastewater is considered as one of the most significant environmental challenges since it is hard to degrade naturally containing various pollutants such as complex dyes, heavy metals, and chemical additives [1, 2]. Textile discharges contain a complex mixture of dyes, heavy metals, and organic compounds, which have long been recognized as severely detrimental to both the quality of water bodies and drinking water. [3]. The complications associated with dyes in textile wastewater are attributed to their non-biodegradable properties. Dyes resist treatment by standard technologies, impart color to receiving rivers, and may inevitably cause toxicity. Furthermore, on a global scale, the volume of textile wastewater continues to increase. It is estimated that the textile industry uses approximately 3×10^3 m^3 of water daily to manufacture 20 tons of textiles [4]. Textile wastewater can be acidic or alkaline depending on the dyeing process, making it more difficult to treat. Textile effluents may cause cancer and mutations in humans. Therefore, separating dyes from textile effluent requires appropriate treatment methods [5]. Amongst dye removal technologies, nanofiltration (NF) is now recognized as an efficient membrane-based method for dye removal from wastewater due to its selective separation characteristics at the nanoscale scale [6], [7], [8]. Because of its enhanced permeate flux, wide retention ranges from 100 to 1000 Da, and inexpensive preliminary investment in the middle ground between reverse osmosis (RO) and

*Corresponding author e-mail: m.bassyouni@eng.psu.edu.eg..

Receive Date: 11 June 2024, Revise Date: 23 June 2024, Accept Date: 11 July 2024

DOI: 10.21608/ejchem.2024.296854.9846

©2024 National Information and Documentation Center (NIDOC)

ultrafiltration (UF), nanofiltration (NF) has attracted attention from both academia and industry [9], [10], [11]. Biopolymers have recently gained importance for membrane applications due to their superior sustainability, low cost, toxicity-free, excellent film-fabrication ability, and ease of accessibility [12]. One of the main biopolymers used in the fabrication of membranes for textile wastewater treatment applications is chitosan (CS). Due to its remarkable capacity for film formation, potent hydrophilicity, non-toxicity, enhanced antibacterial activity, and distinct biodegradability attributes [13], [14]. The reactive amino and hydroxyl groups of chitosan give it multifunctional properties. Additionally, these functional groups support the hydrophilic properties of CS, which enhance sorption and high-water diffusion [15], [16]. Among its drawbacks are low porosity, limited mechanical strength, and weaker stability. By adding specific fillers, such as SiO_2, TiO_2, graphene oxide, and polyethylene glycol, the properties of the CS membrane are enhanced for wastewater treatment [17], [18], [19].

Polymeric nanofiltration membranes, encompassing polysulfone (PSF), polyamide (PA), and polyvinylidene fluoride (PVDF) materials, have been extensively researched and employed in many uses. These membranes have adjustable surface characteristics, strong mechanical strength, and chemical stability. Nevertheless, they frequently have drawbacks such as poor fouling resistance, hydrophobicity, lack of biocompatibility, and restricted selectivity for particular solutes [20]. On the other hand, chitosan-based nanofiltration membranes have attracted a lot of interest because of their special qualities, which include ease of functionalization, affordability, biocompatibility, and environmental sustainability. Furthermore, chitosan may have several drawbacks, including pH sensitivity and poor mechanical stability. Chitosan-based membranes can be enhanced for a variety of applications, providing long-term and economically viable water treatment solutions, by overcoming these challenges through suitable material modifications, surface treatments, and operational considerations [21].

Several investigations have examined the potential of chitosan membranes for nanofiltration applications, particularly in the treatment of textile wastewater [22], [23], [24]. It was reported that the prepared CS membranes having an appropriate thickness and enhanced mechanical properties have significant permeate flux and removal percentages of up to 99% for six types of common dyes in textile effluent and permeation flux up to 2.17 Lm-2h-1 [15]. Long-term study of dye separation shows greater stability of the CS membrane. However further studies are required to improve the filtration performance of CS membranes by increasing the permeation flux with high rejection rates and low power consumption.

In this study, a neat CS nanofiltration membrane with multi-casting layers was fabricated by a film-casting strategy, the polyester microfiltration membrane was used as a support layer for enhancing the tensile strength. The filtration performance of the fabricated membrane was investigated to examine its ability to reject anionic dyes under differing initial concentrations. Furthermore, the composite membrane properties were investigated in detail through several characterization analysis. Then, the filtration performance of the fabricated membrane in single-component dye solutions was additionally examined to reveal the stability and feasible filtration mechanisms.

This study directly supports several Sustainable Development Goals (SDGs). Removing pollutants from textile effluent improves water quality and sanitation, which aligns with the SDG 6 aims. Furthermore, it contributes to SDG 9 by encouraging innovation and sustainable infrastructure in the textile sector. SDG 12 focuses on reducing the environmental impact of the textile industry through responsible use and production practices. Possible goals and indicators include improving water quality, decreasing pollution, and reducing hazardous waste generation. [4], [25], [26].

2. Materials and methods

Materials

Research reagents such as chitosan (CS > 85% deacetylated) were purchased from Titan Biotech Limited Co. (Delhi, India), and polyethylene glycol (PEG) 380-420 was purchased from Oxford Lab Fine Chem. LLP Co. (Maharashtra, India), sodium hydroxide (NaOH, 99%), and glacial acetic acid (GAA, 99%) were received from Piochem Laboratory Chemicals Co. (Giza, Egypt). The nonwoven support layer (polyester) was purchased from Holykem company, China. The deionized water with conductivity < 2 µS/cm using a reverse osmosis (RO) system. The dye used in this study was direct blue 78 (DB78), which has a relative molecular mass of 1059.95 g/mol, and a solubility of up to 10 g/L at 25 °C [27]. The chemical structure of DB78 dye is shown in Fig. 1.

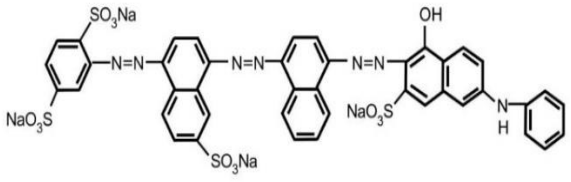

Fig. 1. Chemical structure of direct blue 78 dye.

Fabrication of flat sheet chitosan membrane

The neat CS membrane was fabricated using a multilayer casting technique as illustrated in Fig. 2. The casting solution was spread onto a nonwoven support layer (polyester) using a casting knife, providing a coating thickness ranging from 100 to 500 μm.

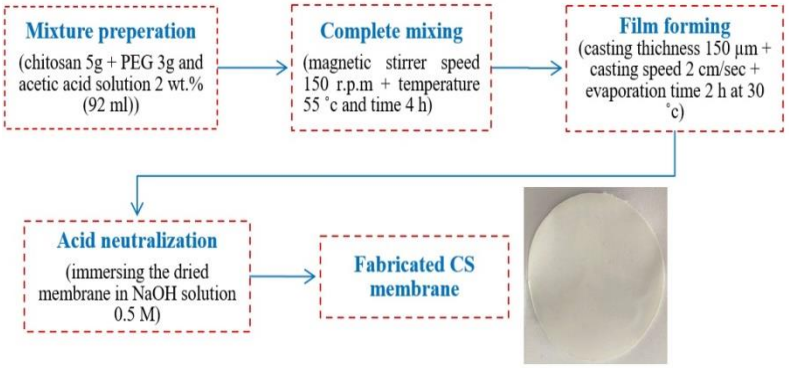

Fig. 2. Graphic illustrate the preparation procedures of CS-based NF membrane.

Concisely, the dried CS (5 g – 5 wt. %), PEG-400 (3 g – 3 wt. %), and 2 wt. % diluted acetic acid solution (92 mL) was added to a 150 mL flask. Furthermore, the components were thoroughly dissolved using magnetic stirring at 55 °C for 4 hours to prepare a homogeneous 5 wt.% chitosan casting solution. The solution was further cooled for 24 hours to reach room temperature for deaeration. Subsequently, a membrane thickness of 150 μm was chosen for the casting process. A stainless-steel plate was positioned horizontally, and the nonwoven support layer (polyester) was placed on the plate. The chitosan (CS) casting solution was poured onto the nonwoven support layer, and the CS wet membrane was then evaporated at 30 °C for 2 hours until the mass remained constant over time, ensuring complete solvent removal. The fabricated chitosan (CS) membrane was labeled as 150-1N, where N denotes the number of layers formed by repeating the casting procedure from 1 to 4 times. To neutralize the acetic acid, the dried membrane was immersed in a 0.5 M NaOH aqueous solution at 25 °C for 24 hours. After removing it from the stainless-steel plate, the CS membrane was washed with deionized (DI) water until reaching a pH of approximately 7.

Characterization of CS Membrane

A TESCAN MIRA field-emission scanning electron microscope (FE-SEM) was used to examine the surface morphology and average thickness of the tested membrane. Before surface analysis, the samples were dried and coated with a 10 nm gold/palladium alloy using a Quorum small sputter coater (SC7620).

Atomic force microscopy (AFM) was used to measure the pristine membrane's surface roughness (Nanosurf FlexAFM). Experiments were conducted in dynamic tapping mode with a notional resonance frequency of 190 kHz and a 7 nm tip. Data on height were gathered throughout a 225 μm^2 sample region.

An optical tensiometer was used to measure the tested membrane's water contact angles. The dried membrane samples were covered with a 5 μL droplet of DI water. Four random spots on each sample were used for the measurements, which were carried out at 25 °C.

The mechanical strengths of the unaltered, altered, and tested membrane were examined using a Zwick/Roell Z010 material testing apparatus. The membrane was cut into strips measuring 2.5 cm by 7 cm and tested until failure. Tensile parameters were determined according to ISO 527-1 standards.

Filtration Performance of CS Membrane

A lab-scale model depicted in Fig. 3 was used to study the filtration performance of the prepared neat CS membrane. The CS membrane cell was designed specifically to examine a flat membrane with an effective 13.85 cm^2 filtration area. With a maximum flow rate of 1.5 L/min, a pressure diaphragm pump powered the feed solution. Before the test, clean water was used to repressurize the membrane for 40 minutes at a transmembrane pressure of 8 bar, or until the water flux achieved a constant value.

.Next, the feed solution was replaced with a single-component synthetic dye solution at two different concentrations: 25 mg/L and 75 mg/L. The water flux ($Lm^{-2}h^{-1}$) was calculated using eq. 1.

$$Jw = \frac{\mathrm{Vp}}{\mathrm{A} \times t \times \Delta \mathrm{P}} \qquad (1)$$

where Vp, at a differential pressure of ΔP (8 bar), is the volume of the permeate solution at test time t (h). The effective membrane area (m^2) for permeability is denoted by (A). Each filtration test took one hour to complete and was conducted at least three times. In the filtering performance test, UV-vis spectroscopy (LaMotte Smart Spectrophotometer, V3 2000-01-MN, USA) was used to assess the concentration of solute that passed from the feed solution into the permeation stream. This was done at the maximum absorption wavelength of 602 nm for the DB78 dye

Using the set concentration of solutions as a basis, the standard calibration curve was used to determine the actual solute concentration in the feed solution.

Eq. 2 was used to determine the CS membranes' rejection rate to DB78 dye throughout the NF procedure.

$$R\ (\%) = \left[\frac{Cf - Cp}{Cf}\right] \times 100 \qquad (2)$$

where C_f (mg/L) and C_p (mg/L) are the concentrations of feed and permeate solutions, respectively.

RESULTS AND DISCUSSION

Filtration performance of CS membrane

The neat CS nanofiltration membranes were evaluated by conducting dye rejection, permeation flux, and antifouling experiments. For DB78 dye rejection, it was observed that the percentage of dye rejection increased with the number of casting layers, reaching an optimum at three casting layers. However, adding more layers beyond this number of layers did not significantly improve dye removal. As shown in Fig. 4, the membranes fabricated with 1, 2, 3, and 4 casting layers exhibited varying removal percentages of 75%, 93%, 100%, and 100%, respectively, for a feed concentration of 25 mg/L. This improvement in removal efficiency can be attributed to a decrease in pore size with increasing the number of casting layers. With increasing the number of casting layers, the rate of solvent evaporation decreases due to the heat isolation effect caused by the previously formed layers. Furthermore, additional layers can be introducing specific functional groups or surface modifications that enhanced the membrane's affinity for dye molecules. These functional groups can facilitate chemical interactions such as adsorption, ion exchange, or complexation, leading to improved dye capture and higher removal percentages.

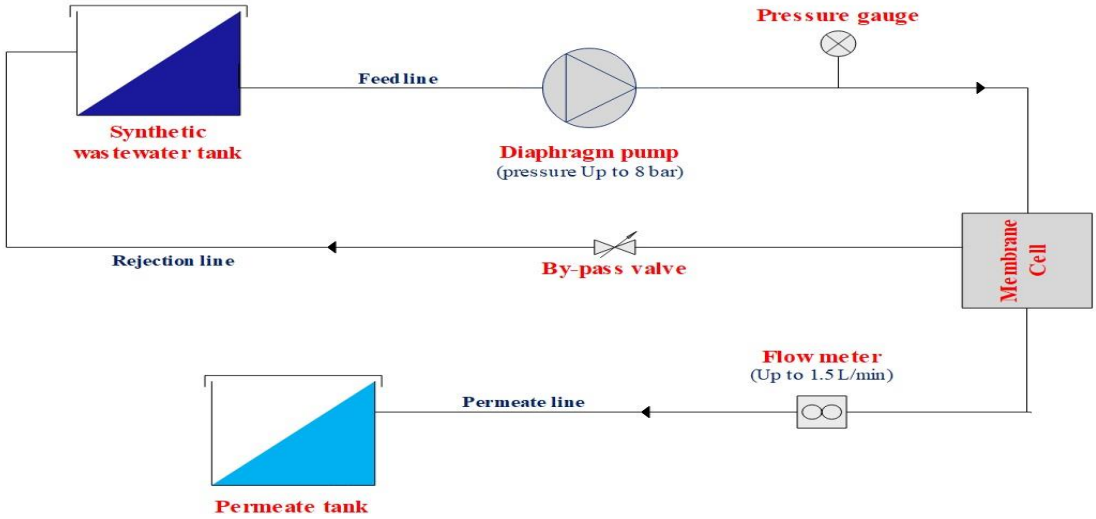

Fig. 3. Schematic drawing for applied treatment process

For permeation flux, it was noted that the relationship between permeation flux and the number of casting layers can vary. Initially, adding more layers may enhance the barrier properties of the membrane, leading to a decrease in permeation flux. However, beyond a certain point (3 casting layers), additional layers did not show a remarkable effect on permeation flux as shown in Fig. 4. The membranes fabricated with 1, 2, 3, and 4 casting layers showed varying flux values of 28.3, 14.2, 7.1, and 6.8 $Lm^{-2}h^{-1}$, respectively, for a feed concentration of 25 mg/L.

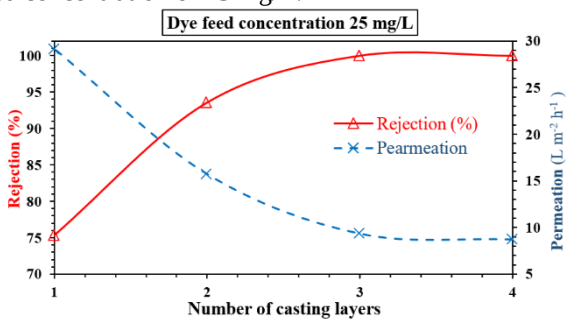

Fig. 4. The effect on number of casing layers on both dye rejection and permeation flux.

This phenomenon can be related to the increase in the overall thickness of the CS membrane due to the increase in the number of casing layers. A thicker membrane offered a longer path for molecules to travel through, leading to a higher probability of interaction with the membrane material and therefore a decreased permeation flux. Furthermore, each casting layer added more polymer material to the membrane. Higher polymer concentration can lead to stronger intermolecular interactions and tighter packing of polymer chains, resulting in a denser membrane structure with reduced permeability.

Fouling is a significant concern in textile wastewater treatment, leading to reduced permeability, increased energy consumption, membrane deterioration, and productivity loss. As shown in Fig. 5, a continuous 6 h nanofiltration test was applied with a dye feed concentration of 25 mg/L under transmembrane pressure 8 bar to investigate the durability of the neat CS nanofiltration membrane.

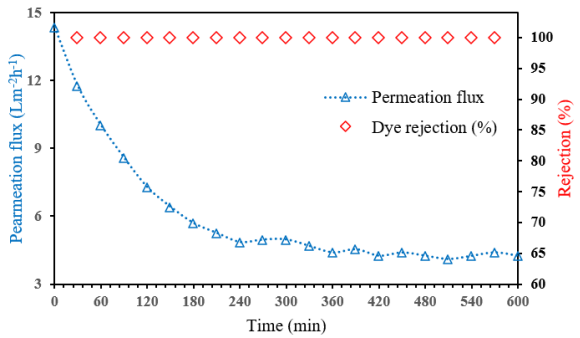

Fig. 5. Stability of CS membrane (3 casting layers) for DB78 dyes removal in a test duration 6 h.

The permeation flow was found to be sharply reduced in the early stages, possibly due to dye absorption on the membrane surface, which led to the formation of a dye cake layer and an increase in osmotic pressure [28, 29]. However, a steady permeation flux of approximately 4.5 $L \cdot m^{-2} \cdot h^{-1}$ could be sustained after the 6-hour test.

Surface morphology of CS membrane

Surface analysis has a critical role in determining the membrane characteristics. The surface morphology of the CS membrane was investigated as shown in Fig. 6. It was observed that the CS membrane obtained by applying 1 casting layer has a rough surface with a large pore size surface which negatively affected the dye removal performance as observed in Fig. 6(a). After applying a multi-layer technique during membrane fabrication, the membrane surface has a superior transformation. As illustrated in Fig. 6(b), it was converted into a smooth surface with an enhanced pore structure having a small radius. This change in membrane surface morphology was successful in achieving high removal performance for dyes. Smooth-surface membranes can exhibit high performance in applications where high throughput is critical, such as water treatment or industrial processes. The obtained surface morphology is attributed to the reduction in solvent evaporation rate resulting from the multilayer coating technique used in the fabrication process. With each increase in the number of casting layers, the previously formed layers act as insulating barriers for liquid evaporation.

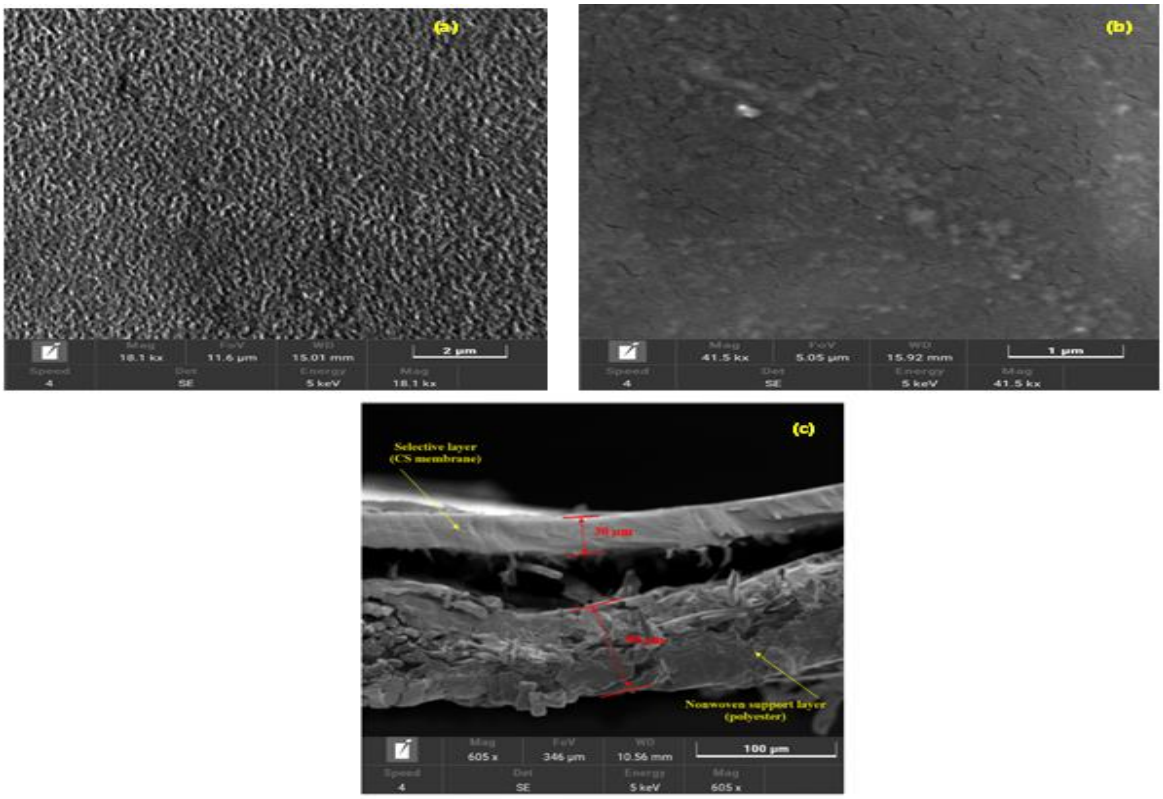

Fig. 6. SEM analysis: (a) CS membrane surface morphology, (b) Cross-section thickness measurements.

This heat isolation increased with an increase in casting layers, thereby reducing the rate of solvent evaporation and resulting in a smooth surface morphology. When the solvent evaporates rapidly; the membrane material contracts, resulting in surface irregularities such as wrinkling or crumpling. These variations in surface texture adversely affect important properties such as surface area, roughness, and porosity. During the filtration process, the thick selective skin layer depicted in Fig. 6(c) acted as a barrier for DB78 dye removal. Moreover, the inner multilayers created pathways for water molecule transport. Ultimately, the adjusted morphology supported high permeation flux, excellent separation efficiency, and antifouling performance for textile wastewater treatment [10].

Surface roughness of CS membrane

To investigate the CS membrane surface roughness, the AFM analysis was conducted as shown in Fig. 7. It was observed that the neat CS membrane displayed a low surface roughness (R_a= 13.06 nm and R_q= 15.4 nm) with heightened rigid-valley structure.

The reduced surface roughness was attributed to the multiple casting layers applied during the membrane fabrication process, which enhanced this effect. Each subsequent layer helped to correct surface imperfections or defects from the previous layer, resulting in a smooth and defect-free surface and minimizing membrane roughness. Multiple casting layers enable better control over membrane thickness and morphology. Depositing several thin layers allowed for achieving a more uniform membrane thickness and pore size distribution, thereby further reducing surface roughness[30].

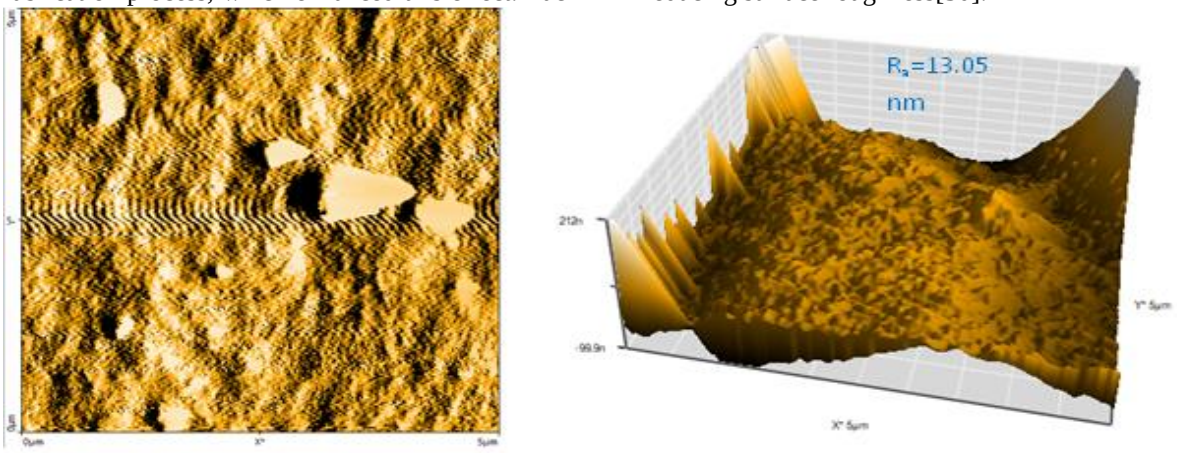

Fig. 7. AFM analysis for the neat CS membrane.

Mechanical testing of CS membrane

The mechanical stability of the neat CS membrane in terms of stress-strain curve was investigated as shown in Fig. 8. The CS nanofiltration membrane possessed a typically superior mechanical stability with an ultimate tensile strength equal to 55 MPa (before filtration test) compared to 44 MPa for CS membrane after 600 min filtration along with the elongation at break of about 24.6 %. These findings highlight the critical role of the nonwoven support layer in enhancing the mechanical stability of the neat CS membrane. A mechanically stable membrane can endure the stresses and pressures encountered during filtration processes without experiencing deformation or breakage. This resilience ensures prolonged operational life and diminishes the requirement for frequent replacements, thereby reducing overall maintenance costs [31].

.

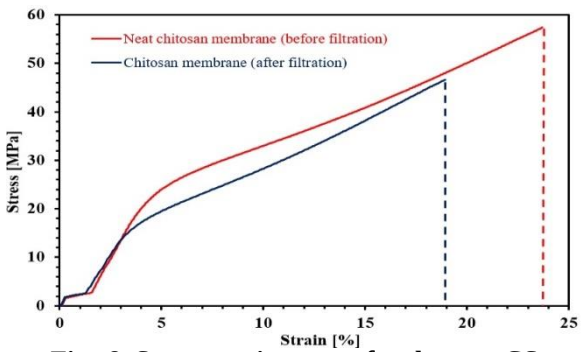

Fig. 8. Stress-strain curves for the neat CS membrane and nonwoven support layer.

Wettability of CS flat sheet membrane

Contact angle measurements were conducted to investigate the wettability of the CS nanofiltration membrane, which plays a crucial role in membrane characterization, as shown in Fig. 9. It was observed that increasing the number of casting layers during membrane fabrication enhanced the hydrophilicity of the CS membrane. Specifically, increasing the number of casting layers from 1 to 3 resulted in a significant decrease in contact angle from 96.4˚ to 80.3˚ (less than 90˚). These results indicate the enhanced hydrophilicity of the fabricated CS membrane. Furthermore, it enhanced the wetting ability which led to better contact between the feed solution and the membrane surface, resulting in improved separation efficiency and higher flux rates. Hydrophilic membranes typically have higher surface energy compared to hydrophobic membranes. This higher surface energy promotes interactions with polar molecules and aqueous solvents, which can be beneficial in applications such as membrane-based separations, where specific interactions between the membrane and target molecules are desired for selective permeation [32].

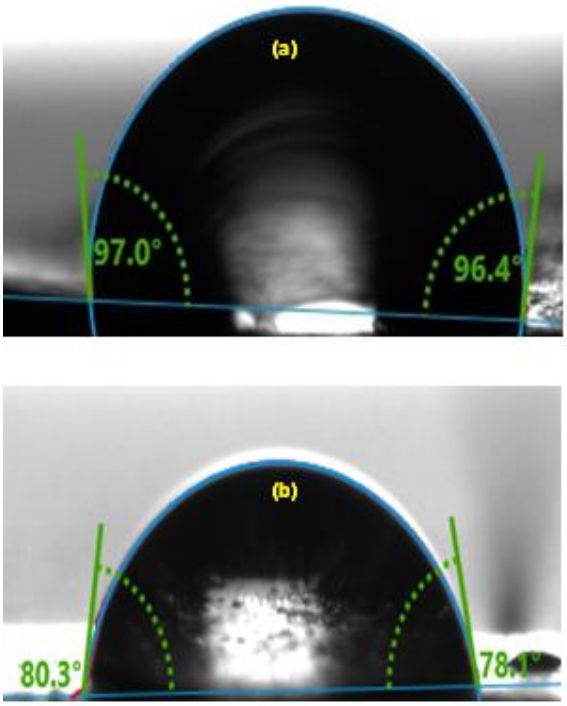

Fig. 9. Contact angle measurements for (a) the neat CS membrane (1 casting layer) and (b) the neat CS membrane (1 casting layer).

Several issues need to be addressed for the successful application of the fabricated chitosan membranes on an industrial scale such as; scalability of fabrication processes, and scaling-up membrane fabrication processes from laboratory to industrial scale. These issues can present challenges related to maintaining product quality, consistency, and cost-effectiveness. Optimizing fabrication methods, equipment, and workflow to ensure scalability while meeting performance requirements is crucial. Material sourcing and cost; large-scale production of chitosan membranes requires a reliable supply of raw materials at a reasonable cost. Ensuring consistent quality and availability of chitosan from sustainable sources is essential for sustainable industrial production. Process efficiency and throughput; industrial-scale membrane production must achieve high throughput and efficiency to meet demand while minimizing production costs. Optimizing process parameters, equipment utilization, and production workflows is necessary to enhance efficiency and productivity.

3. CONCLUSION

The neat CS nanofiltration membranes are simply fabricated using the film casting strategy, the membranes with a significant anionic dye separation performance, and high permeation flux have been successfully fabricated. The effect of several casting layers on CS membrane performance and permeability was studied. On increasing the number of casting layers from 1 to 4, the dye rejection percentage increased from 75% to 100% leading to the resultant nanofiltration membrane with a high dye rejection performance. The hydrophilic prepared CS membrane with a 3-casting layer having a 30 µm selective layer thickness, and average surface roughness Ra= 13.06 nm. The ultimate tensile strength of the CS membrane was decreased from 55 MPa to 44 MPa after a 600 min filtration test with a reduction percentage of 20 % which indicates superior mechanical behavior. This study demonstrates how easily and affordably neat CS membranes can be fabricated using the recently established multistep film coating process, which has potential applications in the removal of anionic dyes from textile effluent.

4. Acknowledgment

The researchers would like to acknowledge the assistance provided by the Science and Technology Development Fund (STDF) for funding project, No. 41902 (Center of Excellence in Membrane-based Water Desalination Technology for Testing and Characterization).

5. References

[1] S. S. Chakraborty, Engineering Solutions for Sustainable Development. 2023. doi: 10.2749/newdelhi.2023.0021.

[2] M. M. H. Elzahar and M. Bassyouni, “Removal of direct dyes from wastewater using chitosan and polyacrylamide blends,” Sci. Rep., vol. 13, no. 1, pp. 1–16, 2023, doi: 10.1038/s41598-023-42960-y.

[3] A. Eteba, M. Bassyouni, and M. Saleh, “Utilization of chemically modified coal fly ash as cost-effective adsorbent for removal of hazardous organic wastes,” Int. J. Environ. Sci. Technol., vol. 20, no. 7, pp. 7589–7602, 2023, doi: 10.1007/s13762-022-04457-5.

[4] A. Eteba, M. Bassyouni, A. Mansi, and M. Saleh, “Textile Wastewater Treatment Using a Modified Coal Fly Ash as a Low-Cost Adsorbent,” no. January, pp. 311–324, 2024, doi: 10.1007/978-3-031-46491-1_19.

[5] Zoromba, M. Sh, Mohamed IM Ismail, M. Bassyouni, M. H. Abdel-Aziz, Numan Salah, Ahmed Alshahrie, and Adnan Memic. "Fabrication and characterization of poly (aniline-co-o-anthranilic acid)/magnetite nanocomposites and their application in wastewater treatment." *Colloids and Surfaces A: Physicochemical and Engineering Aspects* 520 (2017): 121-130.

[6] Fouad, Kareem, Mohamed Bassyouni, Mohamed Gar Alalm, and Mamdouh Y. Saleh. "Recent developments in recalcitrant organic

pollutants degradation using immobilized photocatalysts." *Applied Physics A* 127, no. 8 (2021): 612.

[7] Li, Z., Xie, W., Zhang, Z., Wei, S., Chen, J., & Li, Z. (2023). Multifunctional sodium alginate/chitosan-modified graphene oxide reinforced membrane for simultaneous removal of nanoplastics, emulsified oil, and dyes in water. *International Journal of Biological Macromolecules*, *245*, 125524. [8] S. Elhady, M. Bassyouni, R. A. Mansour, M. H. Elzahar, and M. Y. Saleh, "Developed Method for Treatment of Industrial Wastewater from Edible Oil Industry using Membrane Technology," Int. J. Eng. Adv. Technol., vol. 9, no. 3, pp. 3034–3038, 2020, doi: 10.35940/ijeat.c5940.029320.

[9] Mi, Z., Liu, Z., Jin, S., Zhang, D., & Wang, D. (2021). Positively charged nanofiltration membrane prepared by polydopamine deposition followed by crosslinking for high efficiency cation separation. Polymer Testing, 93, 107000.

[10] S. Elhady et al., "Oily wastewater treatment using polyamide thin film composite membrane technology," Membranes (Basel)., vol. 10, no. 5, pp. 1–17, 2020, doi: 10.3390/membranes10050084.

[11] K. J. Diainabo, N. H. Mthombeni, and M. Motsa, "Preparation and Characterization of Hybrids of Cellulose Acetate Membranes Blended with Polysulfone and Embedded with Silica for Copper(II), Iron(II) and Zinc(II) Removal from Contaminated Solutions," J. Polym. Environ., vol. 29, no. 11, pp. 3587–3604, 2021, doi: 10.1007/s10924-021-02094-6.

[12] Li, J., Gong, J. L., Fang, S. Y., Cao, W. C., Tang, S. Q., Qin, M., ... & Wang, Y. W. (2023). Low-pressure thin-film composite nanofiltration membranes with enhanced selectivity and antifouling property for effective dye/salt separation. Journal of Colloid and Interface Science, 641, 197-214.

[13] S. K. Ramachandran and A. Gangasalam, "Reduction of chemical oxygen demand and color from the rice mill wastewater by chitosan/2(5H)-furanone-incorporated ultrafiltration membrane system," Sep. Sci. Technol., vol. 54, no. 3, pp. 409–425, 2019, doi: 10.1080/01496395.2018.1505915.

[14] R. S. M. A. Hamdon, A. Salem, H. G. I. Ahmed, and M. M. H. ElZahar, "Use of Chitosan for Enhancing the Process of Surface Water Purification in Egypt," Int. J. Environ. Sci. Dev., vol. 13, no. 2, pp. 26–34, 2022, doi: 10.18178/ijesd.2022.13.2.1368.

[15] Q. Long, Z. Zhang, G. Qi, Z. Wang, Y. Chen, and Z. Q. Liu, "Fabrication of Chitosan Nanofiltration Membranes by the Film Casting Strategy for Effective Removal of Dyes/Salts in Textile Wastewater," ACS Sustain. Chem. Eng., vol. 8, no. 6, pp. 2512–2522, 2020, doi: 10.1021/acssuschemeng.9b07026.

[16] A. Kovtun et al., "Multifunctional graphene oxide/biopolymer composite aerogels for microcontaminants removal from drinking water," Chemosphere, vol. 259, pp. 1–10, 2020, doi: 10.1016/j.chemosphere.2020.127501.

[17] S. B. Rekik, S. Gassara, J. Bouaziz, A. Deratani, and S. Baklouti, "Enhancing hydrophilicity and permeation flux of chitosan/kaolin composite membranes by using polyethylene glycol as porogen," Appl. Clay Sci., vol. 168, no. December 2018, pp. 312–323, 2019, doi: 10.1016/j.clay.2018.11.029.

[18] X. Qian, N. Li, Q. Wang, and S. Ji, "Chitosan/graphene oxide mixed matrix membrane with enhanced water permeability for high-salinity water desalination by pervaporation," Desalination, vol. 438, no. March, pp. 83–96, 2018, doi: 10.1016/j.desal.2018.03.031.

[19] F. Khoerunnisa et al., "Chitosan/PEG/MWCNT/Iodine composite membrane with enhanced antibacterial properties for dye wastewater treatment," J. Environ. Chem. Eng., vol. 8, no. 2, p. 103686, 2020, doi: 10.1016/j.jece.2020.103686.

[20] S. Karki, G. Hazarika, D. Yadav, and P. G. Ingole, "Polymeric membranes for industrial applications: Recent progress, challenges and perspectives," Desalination, vol. 573, no. November 2023, p. 117200, 2024, doi: 10.1016/j.desal.2023.117200.

[21] R. Borgohain, U. Pattnaik, B. Prasad, and B. Mandal, "A review on chitosan-based membranes for sustainable CO2 separation applications: Mechanism, issues, and the way forward," Carbohydr. Polym., vol. 267, no. September 2020, p. 118178, 2021, doi: 10.1016/j.carbpol.2021.118178.

[22] E. Salehi, P. Daraei, and A. Arabi Shamsabadi, "A review on chitosan-based adsorptive membranes," Carbohydr. Polym., vol. 152, pp. 419–432, 2016, doi: 10.1016/j.carbpol.2016.07.033.

[23] S. R. Mousavi, M. Asghari, and N. M. Mahmoodi, "Chitosan-wrapped multiwalled

carbon nanotube as filler within PEBA thin film nanocomposite (TFN) membrane to improve dye removal," Carbohydr. Polym., vol. 237, no. February, p. 116128, 2020, doi: 10.1016/j.carbpol.2020.116128.

[24] Q. Zia, M. Tabassum, M. Umar, H. Nawaz, H. Gong, and J. Li, "Cross-linked chitosan coated biodegradable porous electrospun membranes for the removal of synthetic dyes," React. Funct. Polym., vol. 166, no. July, p. 104995, 2021, doi: 10.1016/j.reactfunctpolym.2021.104995.

[25] Tóthová, D., & Heglasová, M. (2022). Measuring the environmental sustainability of 2030 Agenda implementation in EU countries: How do different assessment methods affect results. Journal of Environmental Management, 322, 116152.

[26] K. Obaideen, N. Shehata, E. T. Sayed, M. A. Abdelkareem, M. S. Mahmoud, and A. G. Olabi, "The role of wastewater treatment in achieving sustainable development goals (SDGs) and sustainability guideline," Energy Nexus, vol. 7, no. July, p. 100112, 2022, doi: 10.1016/j.nexus.2022.100112.

[27] A. Eteba, M. Bassyouni, and M. Saleh, "Removal of hazardous organic pollutants using fly ash," Environ. Ecol. Res., vol. 9, no. 4, pp. 196–203, 2021, doi: 10.13189/eer.2021.090407.

[28] X. Ma, P. Chen, M. Zhou, Z. Zhong, F. Zhang, and W. Xing, "Tight Ultrafiltration Ceramic Membrane for Separation of Dyes and Mixed Salts (both NaCl/Na2SO4) in Textile Wastewater Treatment," Ind. Eng. Chem. Res., vol. 56, no. 24, pp. 7070–7079, 2017, doi: 10.1021/acs.iecr.7b01440.

[29] E. Alventosa-Delara, S. Barredo-Damas, E. Zuriaga-Agustí, M. I. Alcaina-Miranda, and M. I. Iborra-Clar, "Ultrafiltration ceramic membrane performance during the treatment of model solutions containing dye and salt," Sep. Purif. Technol., vol. 129, pp. 96–105, 2014, doi: 10.1016/j.seppur.2014.04.001.

[30] M. Zhang, K. Guan, Y. Ji, G. Liu, W. Jin, and N. Xu, "Controllable ion transport by surface-charged graphene oxide membrane," Nat. Commun., vol. 10, no. 1, pp. 1–8, 2019, doi: 10.1038/s41467-019-09286-8.

[31] L. Cui et al., "Preparation and characterization of chitosan membranes," RSC Adv., vol. 8, no. 50, pp. 28433–28439, 2018, doi: 10.1039/c8ra05526b.

[32] U. Baig, M. Faizan, and A. Waheed, "A review on super-wettable porous membranes and materials based on bio-polymeric chitosan for oil-water separation," Adv. Colloid Interface Sci., vol. 303, no. February, p. 102635, 2022, doi: 10.1016/j.cis.2022.102635.